9202 *Biochemistry* **2009,** *48,* 9202–9211
DOI: 10.1021/bi901329b

BIOCHEMISTRY
including biophysical chemistry & molecular biology
Article

Detection of Covalent and Noncovalent Intermediates in the Polymerization Reaction Catalyzed by a C149S Class III Polyhydroxybutyrate Synthase[†]

Ping Li,[‡] Sumit Chakraborty,[‡] and JoAnne Stubbe*[,‡,§]

[‡]*Department of Chemistry and* [§]*Department of Biology, Massachusetts Institute of Technology, 77 Massachusetts Avenue, Cambridge, Massachusetts 02139*

Received July 31, 2009; Revised Manuscript Received August 23, 2009

ABSTRACT: Polyhydroxybutyrate (PHB) synthases catalyze the conversion of 3-hydroxybutyryl coenzyme A (HBCoA) to PHB with a molecular mass of 1.5 MDa. The class III synthase from *Allochromatium vinosum* is a tetramer of PhaEPhaC (each 40 kDa). The polymerization involves covalent catalysis using C149 of PhaC with one PHB chain per PhaEC dimer. Two mechanisms for elongation have been proposed. The first involves an active site composed of two monomers in which the growing hydroxybutyrate (HB) chain alternates between C149 on each monomer. The second involves C149 and covalent and noncovalent $(HB)_n$CoA intermediates. Two approaches were investigated to distinguish between these models. The first involved the wild-type (wt) PhaEC primed with sTCoA [a CoA ester of $(HB)_3$ in which the terminal HO group is replaced with an H] which uniformly loads the enzyme. The primed synthase was reacted with [1-^{14}C]HBCoA by a rapid chemical quench method and analyzed for covalent and noncovalent intermediates. Radiolabel was found only with the protein. The second approach used C149S-PhaEC which catalyzes polymer formation at $^1/_{2200}$ of the rate of wt-PhaEC (1.79 min^{-1} vs 3900 min^{-1}). C149S-PhaEC was incubated with [1-^{14}C]HBCoA and chemically quenched on the minute time scale to reveal noncovalently bound [1-^{14}C]$(HB)_2$CoA and $(HB)_3$CoA as well as covalently labeled protein. Synthesized $(HB)_n$CoA (n = 2 or 3) was shown to acylate PhaEC with rate constants of 1−2 min^{-1}, and these species were converted into polymer. Thus, the $(HB)_n$CoA analogues function as kinetically and chemically competent intermediates. These results support the mechanism involving covalently and noncovalently bound intermediates.

Polyhydroxybutyrate (PHB)[1] synthases catalyze the conversion of 3-(*R*)-hydroxybutyryl coenzyme A (HBCoA) to PHBs. These enzymes are representative of a large number of polymerases found in nature which use common, water-soluble metabolites as substrates, require no template, and undergo a phase transition during the polymerization process to form insoluble inclusions or granules (*1*−*6*). PHBs are produced by most bacteria when they find themselves in a nutrient-limited environment and have a readily available carbon source. Up to 95% of the cell dry weight of the organism can be converted into polyoxoesters. When the environment is no longer nutrient-limited, the polymers are degraded by depolymerases, releasing energy and monomers for biosynthesis (*1*, *7*, *8*). PHBs and polyhydroxyvalerates in the appropriate ratio are of general interest as they have properties of thermoplastics and are biodegradable. They can potentially provide an alternative to petroleum-based, nonbiodegradable plastics, if they can be produced in an economically competitive fashion. Many of the proteins involved in biosynthesis and degradation of PHBs have been identified (*8*−*14*). Our efforts have focused on understanding the mechanism of initiation, elongation and granule formation, and termination (*7*, *8*, *15*−*21*). The prototypes for these studies have been the class I synthase from *Ralstonia eutropha* (*22*) and the class III synthase from *Allochromatium vinosum* (*18*, *23*, *24*). In this work, we describe experiments that establish that both covalent and noncovalent intermediates are involved in the polymerization process in the class III synthases.

The class III synthase from *A. vinosum* (PhaEC), isolated from *Escherichia coli*, is composed of a 1:1 complex of two proteins: PhaC (39 kDa) and PhaE (40 kDa) (*23*). PhaC catalyzes the polymerization reaction, while PhaE is not homologous to any protein of known function. However, the presence of PhaE is essential for an active and well-behaved synthase PhaC (*18*). The class III synthase is a tetramer of PhaEC with a small amount of dimer. Both oligomeric states are active. However, it should be noted that the synthase has never been isolated from its host organism.

We have established that the polymerization reaction catalyzed by PhaEC involves covalent catalysis using a catalytic dyad: histidine (H331) and cysteine (C149) (*18*). H331 activates C149 for nucleophilic attack on HBCoA to form an acylated thiol ester intermediate. Ester formation requires an aspartate, D302, which is proposed to function as a general base catalyst in the activation of the hydroxyl group of HBCoA for nucleophilic attack on the

[†]This work was supported by National Institutes of Health Grant GM49171 to J.S. P.L. was supported by NIH Kirschstein-NRSA postdoctoral fellowship F32GM082067.

*To whom correspondence should be addressed. Telephone: (617) 253-1814. Fax: (617) 258-7247. E-mail: stubbe@mit.edu.

[1]Abbreviations: CoA, coenzyme A; HB, hydroxybutyrate; HBCoA, 3-(*R*)-hydroxybutyryl-CoA; $(HB)_2$CoA, dimer of 3-(*R*)-hydroxybutyryl coenzyme A ester; $(HB)_3$CoA, trimer of 3-(*R*)-hydroxybutyryl coenzyme A ester; sT, trimer of 3-hydroxybutyrate in which the terminal hydroxyl is replaced with a hydrogen; sTCoA, saturated trimer CoA; PHB, polyhydroxybutyrate; PhaEC, class III synthase from *Allochromatium vinosum*, PhaC and PhaE coexpressed and copurified; SA, specific activity; S:E ratio, substrate:enzyme ratio; SDS−PAGE, sodium dodecyl sulfate−polyacrylamide gel electrophoresis; wt, wild type; MALDI-TOF MS, matrix-assisted laser desorption ionization time-of-flight mass spectrometry; ESI-MS, electrospray ionization mass spectrometry.

 Published on Web 08/27/2009

Scheme 1: Proposed Mechanisms for PHB Chain Elongation

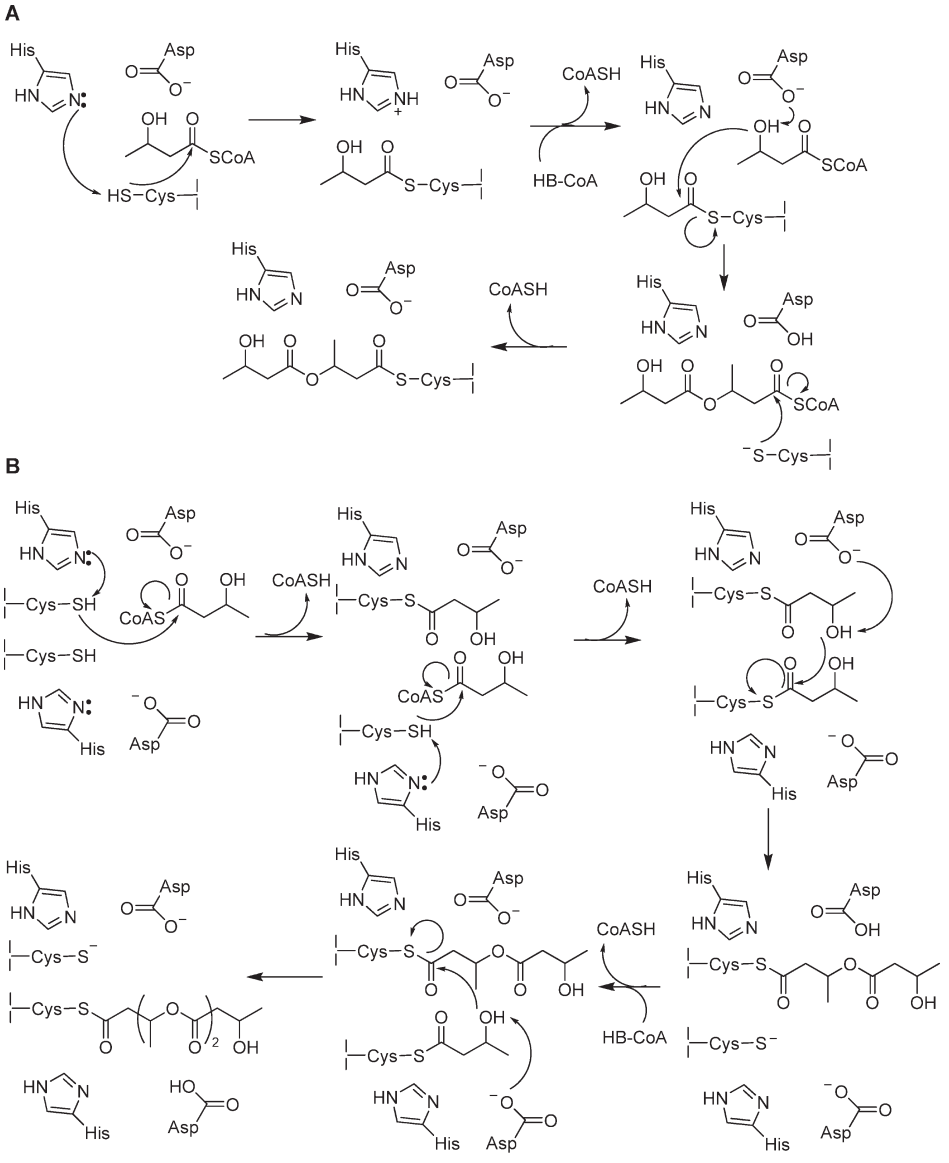

acylated enzyme (*17*, *19*). We have previously proposed two mechanisms for PHB formation. Both involve chain elongation through acylated C149. The mechanism in Scheme 1A proposes that, subsequent to acylation of C149 (HB-PhaC), a second HBCoA reacts with HB-C149 to generate a noncovalently bound $(HB)_2CoA$ that then rapidly reacylates C149. This mechanism is a variant of that proposed for some type III polyketide synthases (*25*). The mechanism in Scheme 1B requires that the active site be at the interface of two PhaC monomers. In this model, the growing $(HB)_n$ chain is always covalently attached to C149 and switches from one monomer to the other upon addition of each subsequent HB unit. This mechanism is a variant of that established for fatty acid synthases in which a cysteine from a ketosynthase and a pantetheinylated thiol attached to the acyl carrier protein are involved in covalent catalysis (*26*).

Efforts to distinguish between the two mechanisms are the focus of this paper. A number of peculiarities associated with PhaEC have made a distinction between the two mechanisms more difficult than might appear at first glance. We have established with both wild-type (wt) class I and III synthases that the rate of elongation is much faster than the rate of initiation and that uniform loading of the protein, essential for studying the elongation process specifically, cannot be achieved (*20*, *22*). Even when the substrate to enzyme (S:E) ratio is 5, a small amount of protein is covalently linked to a huge HB polymer, while most of the protein remains unmodified. To overcome this problem and ensure uniform loading of the synthase, we previously designed "artificial" primers (*21*), such as the saturated trimer CoA (sTCoA), an analogue of $(HB)_3CoA$ in which the terminal hydroxyl group is substituted with a hydrogen. Our previous studies showed that incubation of wt-PhaEC with [^{3}H]sTCoA resulted in the labeling of 0.5 sT per PhaEC based on CoA release (*16*). When the acylated protein, however, was subjected to rapid denaturation, trypsin digestion, and HPLC analysis, three peptides with the same sequence were isolated with trimeric, tetrameric, and pentameric HB units attached to C149 (*18*, *21*). PhaEC was caught in the act of elongation on the basis of the presence of a small amount of HBCoA present in the sTCoA solution due to the fortuitous breakdown of the sTCoA on storage. Thus, our first strategy for distinguishing between mechanisms in Scheme 1 was to use wt-PhaEC acylated with sTCoA followed by rapid mixing with [1-^{14}C]HBCoA and rapid chemical quench (RCQ) methods to look for sT-$(HB)_n$CoA intermediates and PhaC-$(HB)_n$. Only PhaC-$(HB)_n$ was detected,

suggesting that if noncovalent sT-$(HB)_n$CoA intermediates are generated they rapidly reacylate C149.

The second strategy was to examine a variety of PhaEC mutants to find one with a reduced rate of reacylation. The active site serine mutant (C149S) is shown to form PHB with a rate constant of 1.79 min^{-1}, $^1/_{2200}$ the rate of wt-PhaEC (*27*). Studies in which C149S-PhaEC incubated with [1-^{14}C]HBCoA resulted in detection of $(HB)_n$CoA (n = 2 or 3) and $(HB)_n$-C149S-PhaC are presented here. Experiments with synthetically prepared $(HB)_n$CoA (n = 2 or 3) revealed that these noncovalently detected intermediates function in a chemically and kinetically competent fashion. The results together support the mechanism proposed in Scheme 1A involving covalent and noncovalent intermediates.

MATERIALS AND METHODS

Racemic (*R*,*S*)-[1-^{14}C]HBCoA was purchased from American Radio Labeled Chemicals Inc. and was diluted with (*R*)-HBCoA synthesized according to the method of Yuan et al. (*27*). Compounds sTCoA and [^{3}H]sTCoA were synthesized according to Jia et al. (*17*). ESI-MS and MALDI-TOF mass spectra were recorded at the MIT proteomics core facility and MIT biopolymers lab, respectively. RCQ experiments were conducted on an RQF-3 instrument from Kintek. Unless otherwise specified, HPLC was performed using an adsorbosphere nucleoside−nucleotide column (Alltec, 7 μm, 4.6 mm × 250 mm) on a Waters HPLC instrument equipped with a 515 pump and 2996 photodiode array detector. A typical elution protocol used 20 mM KP_i (pH 4.7) (solvent A) and methanol (solvent B) at a flow rate of 1.0 mL/min and a linear gradient of B from 10 to 70% from 0 to 35 min, 70 to 95% from 35 to 45 min, and 95% from 45 to 50 min. Typical recoveries based on scintillation counting were 80−90% of the loaded material.

Purification of Recombinant PHB Synthases. Recombinant wt- and C149S-PhaEC were overexpressed from plasmids pET-UM4 and pET-UM22, respectively, and purified to homogeneity as previously reported (*16*, *18*). Synthases were assayed by the discontinuous method using 5,5′-dithiobis(2-nitrobenzoic acid) (DTNB) to monitor CoA release as previously described (*16*). The specific activities for wt- and C149S-PhaEC were 120 and 0.05 μmol min^{-1} mg^{-1} at 37 °C, respectively.

Reaction of sT-wt-PhaEC with [1-^{14}C]HBCoA. In a total volume of 350 μL, 40 μM wt-PhaEC and 0.52 mM sTCoA in 20 mM KP_i (pH 7.5) and 50 mM NaCl (buffer A) were incubated for 1 min at 37 °C. The sT-wt-PhaEC was immediately loaded into one syringe of the RCQ apparatus and mixed with 2 mM [1-^{14}C]HBCoA [specific activity (SA) = 2000 cpm/nmol] at an S:E ratio of 1 or 50 in the second syringe. At different time points (2.5−1000 ms), the reaction was quenched with 2% $HClO_4$. At the end of the time course, each aliquot was centrifuged and the supernatant was removed and placed on ice. The precipitated protein was washed with H_2O (3 × 75 μL), redissolved in 100 μL of 10% SDS, and analyzed by liquid scintillation counting. The pooled washes were combined with the supernatant, and the pH of the solution was adjusted to ~6.0 by careful titration with 0.5 M NaOH at 4 °C. The solution was then filtered using a Whatman microsyringe filter. The filtration unit was washed with H_2O (3 × 75 μL). The filtrate and washes were combined, concentrated, and analyzed by HPLC. Fractions (1 mL) were collected, and each fraction was analyzed by scintillation counting.

Rate of Acylation of wt-PhaEC by [^{3}H]sTCoA. Using the rapid chemical quench method, 40 μM wt-PhaEC in buffer A was mixed at 37 °C with an equal volume of 0.52 mM [^{3}H]sTCoA (S:E = 13, and SA = 2400 cpm/nmol) in the same buffer. The reaction was quenched with 2% $HClO_4$ at 50 ms, 100 ms, 300 ms, 500 ms, and 1 s. At the end of the experiment, each aliquot was centrifuged and the supernatant was removed. The precipitated protein was washed with H_2O (3 × 75 μL), redissovled in 100 μL of 10% SDS, and analyzed by liquid scintillation counting.

Rate of Acylation of C149S-PhaEC by [^{3}H]sTCoA. The reaction mixture (300 μL) contained 100 μM C149S-PhaEC and 1.3 mM [^{3}H]sTCoA (S:E = 13 and SA = 1278 cpm/nmol) in buffer A and was incubated at 37 °C. At 10, 30, 45, 60, 90, and 120 s, a 40 μL aliquot was withdrawn and quenched with 100 μL of 10% trichloroacetic acid (TCA). The quenched reaction mixtures were centrifuged followed by the removal of the supernatant. The precipitated protein was washed with H_2O (3 × 75 μL), redissolved in 100 μL of 10% SDS, and analyzed by scintillation counting.

Determination of the Kinetic Parameters of HBCoA with C149S-PhaEC. Assays were conducted in a final volume of 200 μL in buffer A containing 20 μM C149S-PhaEC and 50 μM to 6 mM HBCoA. The mixture was incubated at 37 °C, and 20 μL aliquots were removed at various times and quenched with 50 μL of 10% TCA. Each sample was centrifuged to remove the precipitated protein, and then 65 μL of the quenched reaction mixture was added to 70−250 μL of 0.25 mM DTNB in 0.5 M KP_i (pH 7.8) and A_{412} measured. Each substrate concentration was run in triplicate. The kinetic parameters were determined by fitting the data to eq 1.

$$v = \frac{v_{max}[S]}{K_M + [S]} \quad (1)$$

Reaction of [1-^{14}C]HBCoA and C149S-PhaEC Monitored by SDS−PAGE: Coomassie Staining and Autoradiography. In a final volume of 10 μL, 20 μM C149S-PhaEC was incubated with 100 μM to 6 mM [1-^{14}C]HBCoA (SA = 2 × 10^4 cpm/nmol) in buffer A for 60 min at 37 °C. Experiments with S:E ratios of 5, 50, 100, and 300 were conducted. The reactions were stopped by addition of an equal volume of Laemmli buffer with no reducing reagent. Furthermore, the sample was not boiled. From each quenched reaction mixture, 15 μL (12 μg of protein) was loaded onto a 10% SDS−PAGE gel with a thickness of 1.0 mm. The gel was stained with Coomassie for 10 min, destained in fast destain solution for 30 min, transferred to slow destain solution for 15 min, rinsed in H_2O for 1 min, and dried immediately. The dried gels were exposed to the low-energy screen (Molecular Dynamics) for 48 h, scanned using the Storm Imaging System, and analyzed using ImageQuant TL (Amersham Biosciences).

Reaction of [1-^{14}C]HBCoA with C149S-PhaEC at S:E Ratios of 50 or 300: Analysis of Small Molecules by HPLC. In a final volume of 155 μL (at S:E = 50) or 455 μL (at S:E = 300), 20 μM C149S-PhaEC in buffer A was incubated with 1 mM (S:E = 50) or 6 mM (S:E = 300) [1-^{14}C]HBCoA (SA = 2000 cpm/nmol) at 37 °C. Aliquots of 50 μL were withdrawn at different time points and quenched with 50 μL of 2% $HClO_4$. At the end of the time course, the reaction mixture was centrifuged and the supernatant was removed and placed on ice. The precipitated protein was washed with H_2O (2 × 90 μL), redissolved in 100 μL of 10% SDS, and analyzed by liquid scintillation counting. The pooled washes were combined with the supernatant, and the pH was adjusted to ~6.0 by careful titration with

0.5 M NaOH at 4 °C. The neutralized solution was filtered using a Whatman microsyringe filter. The filtration unit was washed with H_2O ($3 \times 80\ \mu L$). The filtrate and washes were combined and analyzed by HPLC. At an S:E ratio of 50, 1 mL fractions were collected. At an S:E ratio of 300, fractions were manually collected at 0−20.0 (1 mL/fraction), 20.0−20.2, 20.2−20.4, 20.4−21.2, 21.2−22.0, and 22.0−50.0 min (1 mL/fraction). Each fraction was analyzed by scintillation counting.

Time-Dependent Inactivation of C149S-PhaEC by $(HB)_2$CoA and $(HB)_3$CoA: Determination of the Rates of Acylation (k_{acyl}) and K_i. In a final volume of 150 μL containing 40 μM C149S-PhaEC and 393 μM to 3.14 mM $(HB)_2$CoA or 686 μM to 2.74 mM $(HB)_3$CoA in buffer A, aliquots (30 μL) were removed and quenched with 20 μL of 10% TCA at various times. Each sample was centrifuged to remove the precipitated protein. Forty-five microliters of the quenched reaction mixture was added to 55 μL of 0.25 mM DTNB in 0.5 M KP_i (pH 7.8), and A_{412} was measured. Values for k_{acyl} and K_i were determined by fitting the data to eq 2

$$\log \frac{[E_a]}{[E]_0} = -\frac{k_{acyl}}{2.3\left(1 + \frac{K_i}{[I]}\right)} t \qquad (2)$$

where $[E]_0$ is the total enzyme concentration, $[E_a]$ is the active enzyme concentration, [I] is the concentration of $(HB)_n$CoA (n = 2 or 3), and t is time.

Isolation of the $(HB)_n$ Acids and $(HB)_n$-C149S-PhaC. In a final volume of 250 μL, 20 μM C149S-PhaEC was incubated with 1 mM [1-^{14}C]HBCoA (S:E = 50, and SA = 2000 cpm/nmol) in buffer A at 37 °C for 60 min. The reaction mixture was then divided into 200 μL (I) and 50 μL (II) aliquots. Aliquot I was immediately transferred to a YM-30 microcentrifuge tube and centrifuged at 14000*g* and 4 °C for 10 min. The protein was washed with buffer A ($2 \times 100\ \mu L$). The protein was then transferred to an Eppendorf tube using 100 μL of buffer A and analyzed by A_{280} and liquid scintillation counting. The filtrate was analyzed by HPLC, and 1 mL fractions were collected and analyzed by scintillation counting. Fractions eluting from 29 to 31 min and from 32 to 43 min were combined and concentrated to ~300 μL using a Speedvac. The pH of the concentrated sample was adjusted to 2 using 2 M HCl before the sample was extracted three times with Et_2O ($3 \times 200\ \mu L$). The organic layers were combined and evaporated to dryness, and the residue was redissolved in 20 μL of MeOH. The aqueous and Et_2O extracts were analyzed by liquid scintillation counting before the material from the Et_2O extract was analyzed by MALDI-TOF using α-cyano-4-hydroxycinnamic acid as the matrix.

Aliquot II was adjusted to pH 2 by addition of 0.5 M HCl before being transferred to a YM-30 microcentrifuge tube and centrifuged at 14000*g* and 4 °C for 10 min. The protein was washed with buffer A ($2 \times 100\ \mu L$). The protein was then transferred to an Eppendorf tube using 30 μL of buffer A. Fifteen microliters of the protein was analyzed by A_{280} and liquid scintillation counting. The rest of the protein (15 μL) was immediately analyzed by ESI-MS performed on the QSTAR Elite quadrupole-TOF mass spectrometer. The sample was diluted to a concentration of 2−3 pmol/μL in water containing 0.1% formic acid and loaded onto the HPLC autosampler. A protein microtrap (Michrom BioResources) was used to bind the protein sample, which was subsequently desalted with water containing 0.1% formic acid and then eluted with a water/acetonitrile mixture (v/v, 1:1) containing 0.1% formic acid for MS analysis.

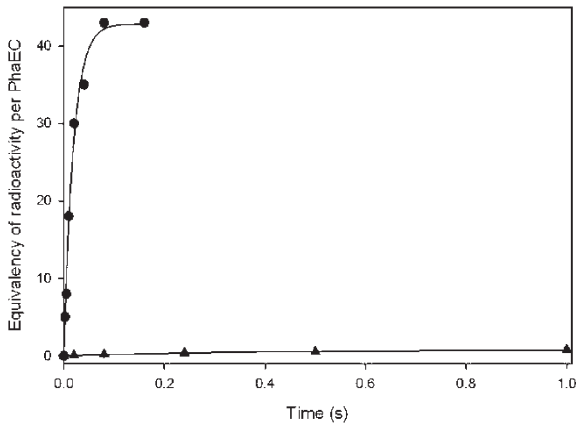

FIGURE 1: Rate of acylation of sT-wt-PhaEC with [1-^{14}C]HBCoA at S:E ratios of 1 and 50. The data are fit to a single exponential using SigmaPlot: (▲) S:E = 1, and $k = 2.4 \pm 0.3\ s^{-1}$, and (●) S:E = 50, and $k = 52.2 \pm 4.4\ s^{-1}$.

RESULTS

Reaction of sT-wt-PhaEC with [1-^{14}C]HBCoA. Our previous studies have shown that with wt synthases the rate of elongation is faster than the rate of initiation (*20*, *22*). Therefore, our first strategy for distinguishing between the two mechanisms depicted in Scheme 1 was to acylate wt-PhaEC with sTCoA. By acylation with sTCoA, the wt-PhaEC is uniformly loaded (0.5 equiv per PhaEC), and thus, the elongation rate can be examined. Wild-type PhaEC was primed with sTCoA at an S:E ratio of 13. Since hydrolysis of sT-wt-PhaEC occurs on the minute time scale ($0.07\ min^{-1}$), this mixture was loaded as rapidly as possible into one syringe of a RCQ apparatus without removing excess sTCoA. The primed synthase was then rapidly mixed with 1 mM [1-^{14}C]HBCoA (S:E = 1 or 50) and then quenched with perchloric acid from 2.5−1000 ms. The precipitated protein was removed and analyzed by scintillation counting, and the supernatant was analyzed by HPLC and scintillation counting. The results of the experiment from analysis of the protein fractions are shown in Figure 1. The PhaEC is acylated with rate constants of $2.4\ s^{-1}$ at an S:E ratio of 1 and $52.2\ s^{-1}$ at an S:E ratio of 50. The rate constant of $52.2\ s^{-1}$ is very similar to the turnover number of $65\ s^{-1}$. Analysis of fractions from the supernatant revealed decreasing amounts of (*R*)-[1-^{14}C]-HBCoA and no evidence of any sT-$(HB)_n$CoA products (lower detection limit is ~3 pmol). At the end of the reaction, (*S*)-[1-^{14}C]HBCoA remained, which is consistent with previously established studies that showed that (*S*)-HBCoA is neither a substrate nor an inhibitor of wt-PhaEC. All of the radioactivity was associated with PhaEC.

Our inability to detect small molecule intermediates in the supernatant prevents us from differentiating between the two mechanisms shown in Scheme 1. If the model in Scheme 1A is valid, then the failure to detect these intermediates could simply indicate that the rate of reacylation of wt-PhaEC by sT-$(HB)_n$-CoA is much faster than its rate of dissociation. Therefore, it is apparent that a mutant enzyme with a decreased rate of reacylation has to be employed to detect the noncovalently bound intermediates should they be generated.

Acylation Rates of [^{3}H]sTCoA with wt-PhaEC and C149S-PhaEC. Our previous studies on a variety of mutants

of PhaEC showed that HBCoA was a substrate for C149S-PhaEC (*16*) with a turnover number that was $^1/_{2200}$ of that of wt-PhaEC. Furthermore, studies of alcoholysis versus thiol ester exchange of thiol esters demonstrate that the rate constant for the former at pH 8 is 50−100-fold slower than the latter (*28*). Thus, we hypothesized that the rate of reacylation of $(HB)_n$CoA analogues with the serine mutant would be greatly reduced compared with that of the wt enzyme and could potentially facilitate the detection of proposed intermediates.

As an indicator of differences in acylation rates, we investigated the rate of acylating wt- and C149S-PhaEC by [^{3}H]sTCoA at an S:E ratio of 13 at 37 °C using RCQ and hand quench methods. Analysis of the radioactivity associated with the precipitated protein ([^{3}H]sT-wt-PhaEC) revealed a rate constant for acylation (k_{acyl}) of 5.12 ± 2.01 s^{-1}. This rate constant is lower than the turnover number of wt-PhaEC (65 s^{-1}) and likely reflects the high K_m for sTCoA and the fact that under the experimental conditions examined, the PhaEC was not saturated with [^{3}H]sTCoA because of its limited availability.

A similar experiment was conducted with C149S-PhaEC under identical conditions (S:E = 13). The analysis of the precipitated protein gave a k_{acyl} of 2.1 ± 0.3 min^{-1} (0.03 s^{-1}). The k_{acyl} of the serine mutant is thus ~170 fold slower than that of the wt. Therefore, as predicted from model reactions, we might be able to use the serine mutant to trap intermediates because of the decreased rate of reacylation.

Determination of Kinetic Parameters for C149S-PhaEC-Catalyzed Polymerization of HBCoA. Our previous studies of wt-PhaEC showed biphasic kinetics for release of CoA from HBCoA. Analysis of the initial rapid phase gave a K_m of 0.130 mM for HBCoA and a k_{cat} of 3900 min^{-1} (*27*). With C149S-PhaEC, HBCoA showed a monophasic release of CoA. The data fitted to eq 1gave a K_m for HBCoA of 1.39 mM and a k_{cat} of 1.79 min^{-1} (Figure S1 of the Supporting Information). From these kinetic parameters, the catalytic efficiency of HBCoA for the wt enzyme ($k_{cat}/K_m = 3.00 \times 10^4$ mM^{-1} min^{-1}) is 20000-fold higher than for the C149S mutant (k_{cat}/K_m = 1.29 mM^{-1} min^{-1}) and k_{cat} is ~2200 times faster than with the serine mutant.

Autoradiography of SDS−PAGE Analysis of the Reactions between wt- and C149S-PhaEC and HBCoA. We have previously monitored chain elongation intermediates generated from reaction of [1-^{14}C]HBCoA with wt-PhaEC at many S:E ratios using SDS−PAGE and autoradiography (*20*). We have repeated these studies for the sake of comparison with the C149S mutant. The results with wt-PhaEC at S:E ratios of 5 and 50 are shown in Figure 2B (lanes 6 and 7). They reveal four regions of radioactivity. The label in region I is proposed to be PhaEC acylated with $(HB)_n$ (n = 3−10). The label in region II is proposed to be associated with $(HB)_n$ (n = 40−100), determined by a comparison of the migratory properties with D302A-PhaEC acylated with HBCoA at an S:E ratio of 100 (*19*). The label in region III is proposed to be predominately tetrameric (320 kDa) with a small amount of dimeric (160 kDa) PhaEC acylated with $(HB)_n$. Region IV is high-molecular mass PHB attached to PhaC that does not enter the gel (*20*). It has to be noted that the gel shown in Figure 2 was run in the absence of mercaptoethanol and without boiling samples before the protein was loaded onto the gel.

To determine if the serine mutant behaves like wt-PhaEC, the same experiment was conducted with [1-^{14}C]HBCoA at S:E ratios of 5, 50, 100, and 300. It must be noted that we used a high enzyme concentration and specific activity of [1-^{14}C]HBCoA in the mutant experiment because wt-PhaEC is 2200-fold more active than C149S-PhaEC. The results of SDS−PAGE analysis with Coomassie staining and autoradiography are shown in panels A and B of Figure 2, respectively. As with wt-PhaEC, most of the mutant remained unmodified on the basis of Coomassie staining (lanes 2−5 in Figure 2A). Autoradiography revealed multiple forms of protein with $(HB)_n$ bound, similar to the observations with the wt enzyme. The tight radiolabel band in region I migrates between PhaC and PhaE in both wt and mutant synthases. The radiolabel associated with the mutant in region I is broader than that with wt and is likely the result of a 3-fold increased protein loading and the higher SA of the [1-^{14}C]HBCoA with the mutant used in the experiment. Species II is assigned to wt-PhaC$(HB)_n$ (n = 40−100). However, with the mutant enzyme, species II has a distinct broad and dark feature that migrates slower than PhaE with a molecular mass in the range of 44−46 kDa. This feature is proposed to be a $(HB)_n$-C149S-PhaC (n = 73 or 75) based on the ESI mass spectrometric analysis presented subsequently. Comparison of the autoradiogram of region II of wt-PhaEC and the serine mutant suggests that the mutant forms shorter PHB chains and appears to be less polydisperse than the wt enzyme. Similar to wt-PhaEC, species III in C149S-PhaEC migrates as a tetramer (320 kDa) with longer $(HB)_n$ chains bound. We propose that the subunits remain associated during PAGE as the samples were not boiled prior to loading. The faster-migrating band in region III, which has been attributed to dimeric PhaEC loaded with PHB, is not detected likely due to a sensitivity issue. Species IV does not enter the gel and corresponds to a small amount of protein associated with the high-molecular mass PHB polymer. Thus, even with the serine mutant, the loading of the substrate is nonuniform and the behavior appears to be similar to that of the wt enzyme. Therefore, studies with this mutant are likely to be representative of the mechanism with wt-PhaEC.

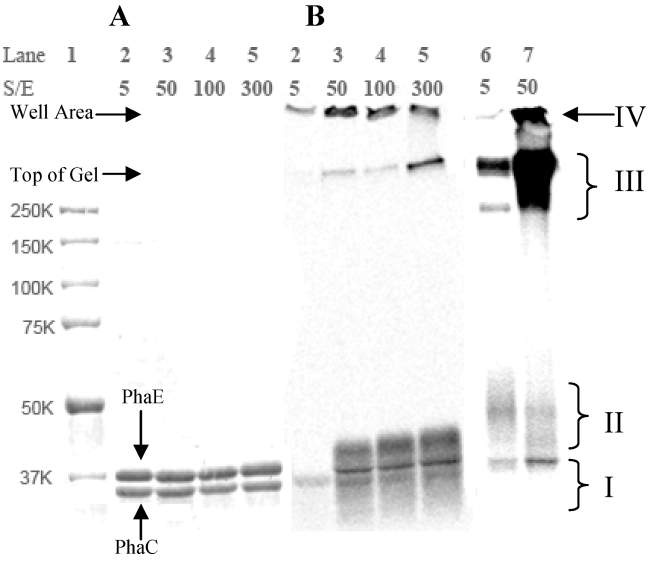

FIGURE 2: SDS−PAGE (10%) monitoring the polymerization catalyzed by C149S-PhaEC (20 μM) and wt-PhaEC (3.3 μM) with [1-^{14}C]HBCoA at the indicated S:E ratios. (A) Lane 1, molecular mass standards; lanes 2−5, Coomassie-stained gel with C149S-PhaEC at S:E ratios of 5, 50, 100, and 300, respectively. (B) Autoradiography of the gel in panel A: lanes 2−5, 12 μg of protein loaded in each lane with SA = 2×10^4 cpm/nmol; lanes 6 and 7, wt-PhaEC (4 μg of protein loaded in each lane) at S:E ratios of 5 and 50, respectively, with SA = 1.1×10^4 cpm/nmol.

Detection of $(HB)_2$CoA and $(HB)_3$CoA in the Reaction between C149S-PhaEC and [1-^{14}C]HBCoA. To look for

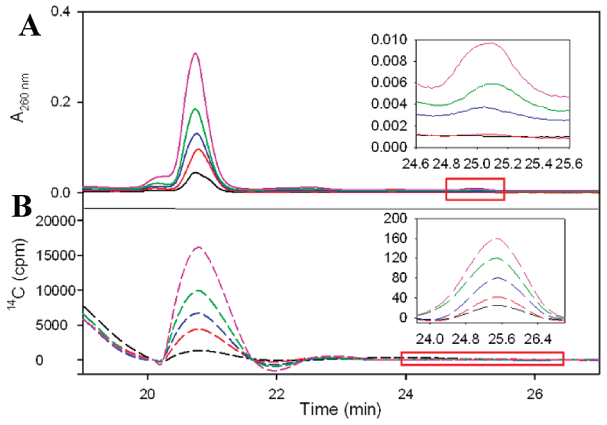

FIGURE 3: HPLC monitoring of the reaction between C149S-PhaEC and [1-^{14}C]HBCoA at 37 °C: (A) A_{260} (solid lines) and (B) radioactivity (dotted lines). The reaction was quenched at 1 (black), 3 (red), 6 (blue), 10 (green), and 15 min (purple) by 2% $HClO_4$. The insets are the expansions of A_{260} and radioactivity features.

$(HB)_nCoA$ intermediates, C149S-PhaEC (20 μM) and [1-^{14}C]HBCoA (6 mM) were incubated at 37 °C and the reaction was monitored by HPLC at A_{260} and scintillation counting (Figure 3). A decrease in the amount of (*R*)-HBCoA [retention time (t_R) of 14.6 min] and an increase in the amount of CoA (t_R = 11.4 min) were observed (data not shown). In addition, two new species with t_R values of 20.8 and 25.1 min were observed, and analysis by scintillation counting revealed both species were radiolabeled (Figure 3).

The new species were isolated, concentrated, and characterized by MALDI-TOF mass spectrometry. The results are shown in Figure 4. The calculated mass of $(HB)_2CoA$ in the negative mode is 938.18 Da. The observed masses of the species with a retention time of 20.8 min are 938.02 and 961.97 Da. These masses are consistent with $(HB)_2CoA$ $(M - H)^-$ and $(M - H + Na)^-$ ions, respectively. Since MALDI-TOF mass spectroscopy uses soft ionization, decomposition of $(HB)_2CoA$ is not expected. However, a small peak with a mass of 833.98 Da was observed, which corresponds to crotonyl-CoA with a calculated mass of 834.13 Da for the $(M - H)^-$ ion. This species could be produced by elimination of HB from $(HB)_2CoA$ (Scheme 2). Moreover, as shown in Figure 4, there is a peak at A_{260} with a t_R of 20.3 min just prior to elution of $(HB)_2CoA$, which might be associated with crotonyl-CoA.

The calculated mass of $(HB)_3CoA$ is 1024.22 Da. The compound with a t_R of 25.1 min has observed masses of 1024.12 and 1047.89 Da, corresponding to the $(M - H)^-$ and $(M - H + Na)^-$ ions, respectively, of $(HB)_3CoA$. Further confirmation of the identity of the species with t_R values of 20.8 and 25.1 comes from their respective coelution with chemically synthesized $(HB)_2CoA$ and $(HB)_3CoA$ as described in Scheme S1 of the Supporting Information.

Determination of the Rate Constants for Acylation of C149S-PhaEC by $(HB)_2CoA$ and $(HB)_3CoA$ Supports Kinetic Competence in HBCoA Polymerization. We have previously reported that $(HB)_2CoA$ and $(HB)_3CoA$ function in vitro as primers of class I PhaC from *R. eutropha* (*21*). However, their detailed syntheses have not been reported. To confirm the identity of the new CoA analogues detected during the turnover of C149S PhaEC and to help establish the kinetic competence of their formation, $(HB)_2CoA$ and $(HB)_3CoA$ were synthesized. The detailed protocol is described in Scheme S1 (Supporting Information) as is their characterization.

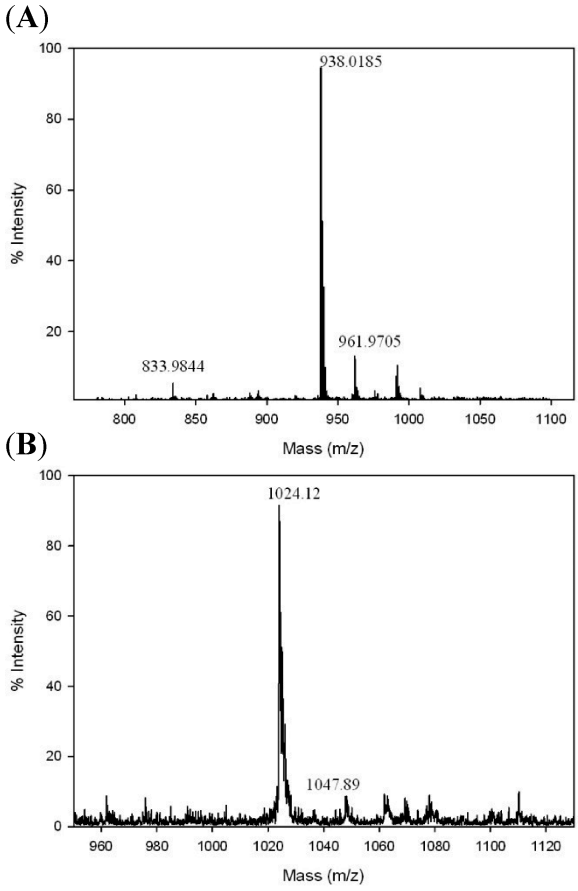

FIGURE 4: MALDI-TOF mass spectra of $(HB)_nCoA$ intermediates (Figure 3) in negative ion mode: (A) peak (Figure 3) at 20.8 min [$(HB)_2CoA$] and (B) peak at 25.1 min [$(HB)_3CoA$].

Scheme 2: Proposed Formation of Crotonyl-CoA Corresponding to the Peak at 20.3 min in Figure 3

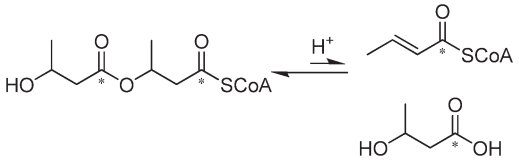

Scheme 3: Single-Turnover Reaction between PhaC and $(HB)_nCoA$ ($n \geq 2$)

$$E + (HB)_nCoA \rightleftharpoons E \cdot (HB)_nCoA \longrightarrow E\text{-}(HB)_n + CoA$$

Both $(HB)_2CoA$ and $(HB)_3CoA$ are mechanism-based inhibitors that can acylate C149S-PhaEC (Scheme 3). To determine the dissociation constant (K_i) for binding of $(HB)_nCoA$ to C149S-PhaEC and k_{acyl}, $(HB)_nCoA$ (n = 2 or 3) was incubated at various concentrations with C149S-PhaEC and aliquots were removed as a function of time and quenched with 10% TCA to measure CoA release. The results of the analysis using eq 2 are shown in Figure 5A,B. The K_i for $(HB)_2CoA$ is 2.02 mM with a k_{acyl} of 1.1 min^{-1}. Similar experiments with $(HB)_3CoA$ gave a K_i of 1.54 mM and a k_{acyl} of 2.35 min^{-1}. The rate constant for production of PHB by C149S-PhaEC is 1.79 min^{-1}, thus, both of these oligomers are capable of being involved in polymer formation in a kinetically competent fashion.

Rate of Formation of $(HB)_2CoA$ and $(HB)_3CoA$ by C149S-PhaEC. Kinetic competence implies not only that the

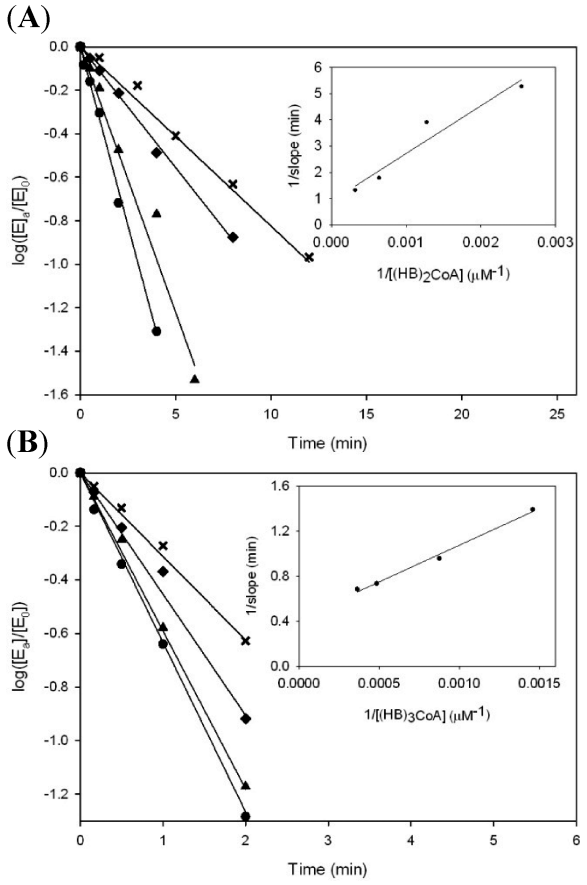

FIGURE 5: Time-dependent inactivation of C149S-PhaEC with $(HB)_2CoA$ (A) and $(HB)_3CoA$ (B). (A) $(HB)_2CoA$ concentrations of 393 (×), 785 (◆), 1570 (▲), and 3140 μM (●). (B) $(HB)_3CoA$ concentrations of 686 (×), 1143 (◆), 2058 (▲), and 2744 μM (●). The insets are the secondary reciprocal plots of slopes vs inhibitor concentration.

rate of utilization of $(HB)_nCoA$ is greater than or equal to the rate of polymer formation but also that their rate of formation must be faster than the overall rate of the reaction. To examine this rate, C149S-PhaEC (20 μM) was incubated with [1-^{14}C]HBCoA (6 mM) and the reaction progress was monitored by HPLC for $(HB)_2CoA$ and by scintillation counting for $(HB)_n$-C149S-PhaEC subsequent to protein isolation by filtration (Figures 3 and 6). Intermediate $(HB)_2CoA$ was formed at a rate constant of 0.30 min^{-1} and $(HB)_n$-C149S-PhaC at a rate of 1.61 min^{-1}. The reaction rate is thus 2.21 min^{-1} and is similar to that detected for release of CoA from HBCoA (1.79 min^{-1}). The relative rates of reacylation versus $(HB)_nCoA$ dissociation appear to be ~2.7:1. Thus, the kinetics reveal that $(HB)_2CoA$ can function as an intermediate in polymer formation. Given the relative rates of acylation by C149 versus S149, it seems reasonable that our inability to detect this intermediate with wt synthase is due to its enhanced reacylation as we proposed.

A similar analysis for $(HB)_3CoA$ could not be conducted because of the low levels of material. The apparent slow rate of formation of $(HB)_3CoA$ and the inability to detect $(HB)_nCoA$ ($n \geq 4$) may be related to the slow rate constants for dissociation of longer HB chains, and hence, the ratio of reacylation to dissociation increases.

Detection of $(HB)_n$ Acids by HPLC at Long Incubation Times with C149S-PhaEC. In an experiment designed to monitor the formation and disappearance of $(HB)_2CoA$ and $(HB)_3CoA$, a reaction of C149S-PhaEC with [1-^{14}C]HBCoA at

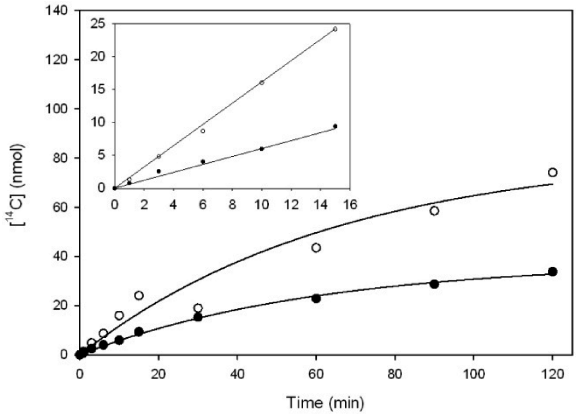

FIGURE 6: Rate of formation of $(HB)_2CoA$ (●) and $(HB)_n$-C149S-PhaEC (○). The reaction was conducted with 20 μM C149S-PhaEC and 6 mM [1-^{14}C]HBCoA in 50 μL of buffer A. The inset is the expansion of the linear portion of the progress curve (0−16 min).

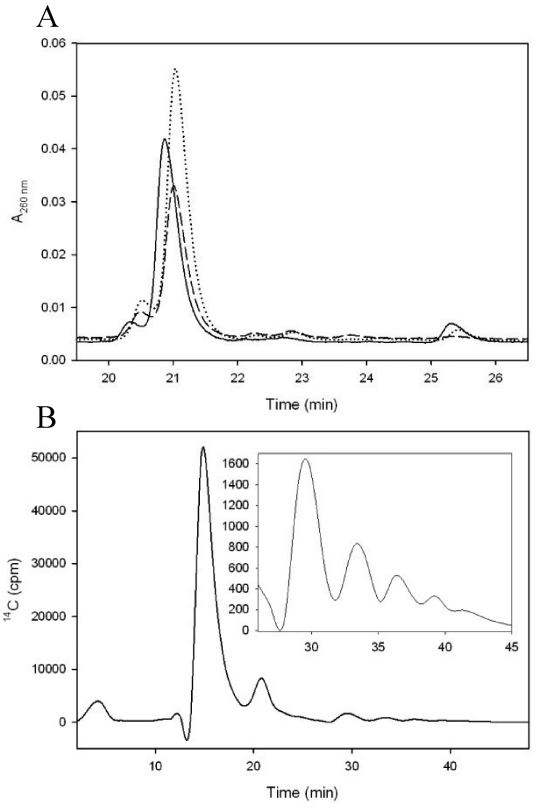

FIGURE 7: Reaction between 20 μM C149S-PhaEC and 1 mM [1-^{14}C]HBCoA (S:E = 50). (A) The reaction was acid-quenched at 10 (—), 30 (···), and 60 min (---) and monitored by A_{260}. (B) Radioactivity profile of the reaction at the 60 min time point. The reaction was not quenched with acid. The inset is the expansion of the 25−45 min region.

an S:E ratio of 50 was monitored by A_{260} and scintillation counting over 60 min. As depicted in Figure 7A, where the changes in A_{260} were monitored, $(HB)_2CoA$ production increased during the first 30 min and then decreased while production of $(HB)_3CoA$ only decreased. Examination of a similar reaction at 60 min revealed that while ~50% of the radioactivity was associated with $(HB)_2CoA$, ~25% eluted between 29 and 43 min with limited A_{260}. Our studies of the stability of sT-wt-PhaEC indicated that the acid of the sT was formed with a rate constant of 0.07 min^{-1}. Thus, given

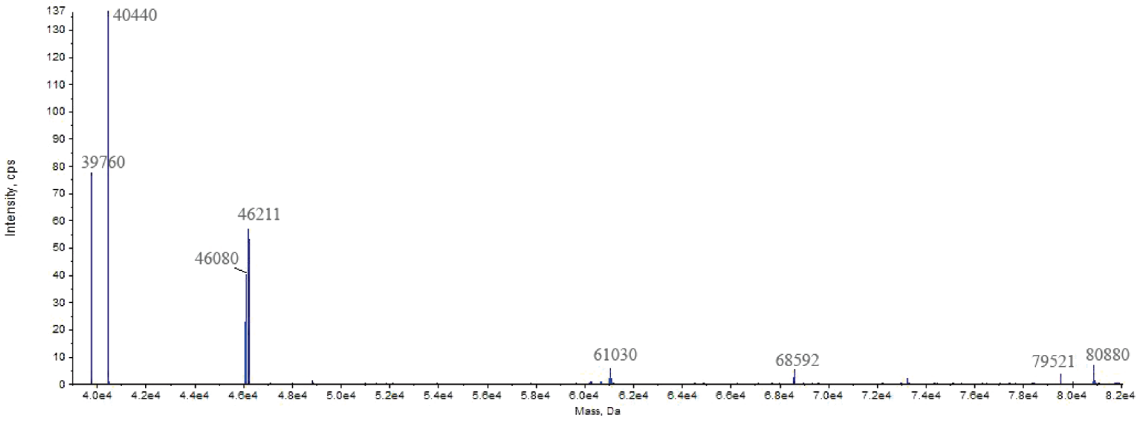

FIGURE 8: Deconvoluted ESI-MS spectrum of C149S-PhaEC modified with PHB.

Table 1: Assignments of the Peaks in the ESI-MS Spectrum of the Modified Protein

observed mass (Da)	HB units	calculated mass (Da)	assignment
39760		39759	C149S-PhaC
40440		40440 (without Met)	H313R/S314D-PhaE
46080	73	39759 + 86.04 × 73 + 39(K) = 46079	C149S-PhaC-73mer
46211	75	39759 + 86.04 × 75 + 1 = 46213	C149S-PhaC-75mer
61030	247	39759 + 86.04 × 247 + 23(Na) = 61034	C149S-PhaC-247mer
68592	334	39759 + 86.04 × 334 + 39(K) × 2 + 23(Na) − 2 = 68595	C149S-PhaC-334mer
79521		79518	$(C149S\text{-}PhaC)_2$
80880		80880	$(H313R/S314D\text{-}PhaE)_2$

the long incubation times, we postulated that the radioactivity eluted between 29 and 43 min was likely associated with oligomers of hydroxybutyric acids $(HB)_nCO_2H$.

Knowing the distribution of *n* might be informative about the optimal length of the primer and the size of the $(HB)_n$ associated with region I of the SDS gel (Figure 2). If the products that eluted between 29 and 43 min (Figure 7B) are $(HB)_nCO_2H$, then acidification of the solution to pH 2 should allow them to be extracted into diethyl ether. Fractions from 29 to 31 min and from 32 to 43 min were pooled separately and examined by this procedure. For the fraction from 29 to 31 min, 90% of the radioactivity was extracted and analysis of this material by MALDI-TOF in the positive mode revealed masses consistent with $(HB)_nCO_2^-$ as the Na/K salt, where $n = 4$ or 5 (Figure S2 of the Supporting Information). Extraction of fractions from 32 to 43 min resulted in 73% of the radioactivity recovered in the ether layer, and MALDI-TOF analysis revealed oligomeric acids where $n = 6$, 7, or 8 as Na/K salts (Figure S3 of the Supporting Information). As described in Materials and Methods, 4 nmol of PhaEC was incubated with 200 nmol of HBCoA and 50 nmol of radiolabeled material was eluted between 29 and 43 min by HPLC analysis. The sizes of the $(HB)_n$ acids detected and the previously measured rate of hydrolysis of sT-PhaEC suggest that during the 60 min experiment it is reasonable that acids might be detected. Moreover, the results suggest that the acids might be indicative of the acylated PhaC in region I of the gel (Figure 2) and indicative of a primed enzyme.

Characterization of the PHB Chain Length Attached to the Protein by ESI-MS. In an effort to establish the range of *n* for $(HB)_n$ attached to the protein, the reaction between C149S-PhaEC and [1-^{14}C]HBCoA at the 60 min time point was acidified to pH 2 to stop the reaction and minimize hydrolysis of the acylated enzyme. The protein was separated from small molecules using a YM-30 microcentrifuge tube and was immediately analyzed by ESI-MS. The results are shown in Figure 8. Tentative assigments of mass to structure are summarized in Table 1. The species at 39760 and 40440 Da correspond to C149S-PhaC and PhaE (a mutant with two mutations relative to wt), respectively. The other species with masses of 46080 and 46211 Da have been assigned to $(HB)_n$-C149S-PhaC, where *n* is 73 and 75, respectively. We propose that $(HB)_{73}$-C149S-PhaC and $(HB)_{75}$-C149S-PhaC might be the dark band observed in region II in SDS−PAGE analysis (Figure 2). The masses attributed to $(HB)_n$-C149S-PhaC ($n = 247$ and 334) might migrate in the region of species III in the corresponding autoradiography gel.

DISCUSSION

We have proposed two mechanisms for PHB polymerization catalyzed by PhaEC (Scheme 1A,B) on the basis of the available information. The mechanism in Scheme 1B is less appealing as it requires that the active site be at the interface of two monomers and that each monomer contribute a single cysteine involved in covalent catalysis. No structures of the class I or III synthases are available. However, all synthases possess a lipase box, and threading models suggest that the synthase is an α,β-hydrolase superfamily member with the active site nucleophile at the elbow of a strand turn helix (*16*, *29*). Lipases are in general monomers, and their active sites are deeply buried, requiring a moderately long tunnel for access of their triacylglycerol substrates. Given this information, it is thus difficult to see how two deeply buried active sites, one from each PhaC monomer, could generate the required active site at their interface. Moreover, earlier attempts failed to trap the second covalent intermediate using potential chain terminators such as 3-methoxy- and 3-fluoro-butyryl-CoA (*15*). Addition of the terminator to the preacylated class I

enzyme (sT-PhaC) did not release any detectable CoA and thus failed to provide support for a second covalent intermediate.

The mechanism shown in Scheme 1A is based on some type III polyketide synthases (*25*) and requires only one active site nucleophile. According to this model, it predicts 2 equiv of sT per dimer of PhaEC, in contrast with the experimental observations. However, similar phenomena of half-site reactivity have been observed with the homodimers of chalcone synthase (*30*) and prenyltransferases (*31*), where multiple reaction steps occur within a single reactive site.

Furthermore, the mechanism in Scheme 1A implicating noncovalent intermediates is consistent with our recent studies using an HBCoA substrate analogue in which the CoA was replaced by *N*-acetylcysteamine (NAC and HBNAC) (*32*). This substrate has a turnover number that is $^1/_{100}$ that of HBCoA. The PHB polymers generated from HBNAC are considerably smaller than those generated from HBCoA (75 kDa vs 1.5 MDa) with much higher polydispersity. Furthermore, the C-terminus of the polymer ends with NAC rather than an acid. One interpretation of these observations is that a noncovalent intermediate dissociated from the active site presumably because of the high K_d of PHB-NAC.

The mechanism proposed in Scheme 1A, which predicts noncovalently bound $(HB)_n$CoA intermediates, would likely be difficult to demonstrate with wt-PhaEC, as the enzyme is known to produce polymers of 1.5 MDa with low polydispersity. If intermediates dissociated during the polymerization process, they then would compete with monomer for rebinding and the polydispersity of the PHB would be expected to be high as observed with HBNAC. Thus, our inability to detect sT-$(HB)_n$-CoA analogues by the RCQ approach is not surprising when sT-PhaEC is reacted with HBCoA.

C149S-PhaEC proved to be an ideal candidate for examination of the mechanism of polymerization based on the differences in reactivity of oxygen versus thiol nucleophiles, the slow rate of PHB formation with this mutant, and its similarities to wt-PhaEC in the elongation process (Figure 2). When C149S-PhaEC was reacted with [1-^{14}C]HBCoA, noncovalent intermediates $(HB)_2$CoA and $(HB)_3$CoA along with covalently modified synthase were observed for the first time. These species were demonstrated to be chemically and kinetically competent, providing strong support for the proposed chain elongation mechanism shown in Scheme 1A.

Finally, isolation of $(HB)_nCO_2H$ (n = 4−8), after a long incubation of C149S-PhaEC with HBCoA, might provide us with insight about the priming process catalyzed by PhaEC. These acids are proposed to originate from the hydrolysis of modified C149S-PhaEC corresponding to species I [$(HB)_n$-C149S-PhaC (n = 3−10)] in the autoradiogram (Figure 2B). Thus, our working model holds that the polymer exit tunnel (*20*) may accommodate up to eight HB units. Unfortunately, efforts to detect acylated $(HB)_n$-C149S-PhaC (n = 3−10) by ESI-MS were unsuccessful. However, detection of species tentatively assigned to $(HB)_{73}$-C149S-PhaC or $(HB)_{75}$-C149S-PhaC suggests that as the HB chain grows longer, the rate of hydrolysis of the covalent linkage to PhaC is dramatically reduced. This proposal is consistent with the low polydispersity of the PHB.

In summary, using the active site C149S-PhaEC has allowed detection for the first time of covalently and noncovalently bound HB intermediates. The detailed mechanism of chain extension and termination requires a structure to assess the complexity of this reaction. Efforts with mechanism-based inhibitors to obtain such a structure are in progress.

ACKNOWLEDGMENT

We thank Rachael Buckley for purifying C149S-PhaEC.

SUPPORTING INFORMATION AVAILABLE

Synthesis of $(HB)_2$CoA and $(HB)_3$CoA, kinetic analysis of HBCoA with C149S-PhaEC, and MALDI-TOF mass spectra of $(HB)_nCO_2H$. This material is available free of charge via the Internet at http://pubs.acs.org.

REFERENCES

1. Stubbe, J., Tian, J. M., He, A. M., Sinskey, A. J., Lawrence, A. G., and Liu, P. H. (2005) Nontemplate-dependent polymerization processes: Polyhydroxyalkanoate synthases as a paradigm. *Annu. Rev. Biochem. 74*, 433–480.
2. Cornish, K. (2001) Biochemistry of natural rubber, a vital raw material, emphasizing biosynthetic rate, molecular weight and compartmentalization, in evolutionarily divergent plant species. *Nat. Prod. Rep. 18*, 182–189.
3. Madison, L. L., and Huisman, G. W. (1999) Metabolic engineering of poly(3-hydroxyalkanoates): From DNA to plastic. *Microbiol. Mol. Biol. Rev. 63*, 21–53.
4. Rehm, B. H. A., and Steinbuchel, A. (1999) Biochemical and genetic analysis of PHA synthases and other proteins required for PHA synthesis. *Int. J. Biol. Macromol. 25*, 3–19.
5. Smith, A. M. (2001) The biosynthesis of starch granules. *Biomacromolecules 2*, 335–341.
6. Ugalde, J. E., Parodi, A. J., and Ugalde, R. A. (2003) De novo synthesis of bacterial glycogen: *Agrobacterium tumefaciens* glycogen synthase is involved in glucan initiation and elongation. *Proc. Natl. Acad. Sci. U.S.A. 100*, 10659–10663.
7. Kessler, B., and Witholt, B. (2001) Factors involved in the regulatory network of polyhydroxyalkanoate metabolism. *J. Biotechnol. 86*, 97–104.
8. Rehm, B. H. (2003) Polyester synthases: Natural catalysts for plastics. *Biochem. J. 376*, 15–33.
9. Steinbuchel, A., and Hein, S. (2001) Biochemical and molecular basis of microbial synthesis of polyhydroxyalkanoates in microorganisms. *Adv. Biochem. Eng. Biotechnol. 71*, 81–123.
10. Peoples, O. P., and Sinskey, A. J. (1989) Poly-β-hydroxybutyrate (PHB) biosynthesis in *Alcaligenes eutrophus* H16. Identification and characterization of the PHB polymerase gene (phbC). *J. Biol. Chem. 264*, 15298–15303.
11. Potter, M., Madkour, M. H., Mayer, F., and Steinbuchel, A. (2002) Regulation of phasin expression and polyhydroxyalkanoate (PHA) granule formation in *Ralstonia eutropha* H16. *Microbiology 148*, 2413–2426.
12. Potter, M., Muller, H., Reinecke, F., Wieczorek, R., Fricke, F., Bowien, B., Friedrich, B., and Steinbuchel, A. (2004) The complex structure of polyhydroxybutyrate (PHB) granules: Four orthologous and paralogous phasins occur in *Ralstonia eutropha*. *Microbiology 150*, 2301–2311.
13. Wieczorek, R., Pries, A., Steinbuchel, A., and Mayer, F. (1995) Analysis of a 24-kilodalton protein associated with the polyhydroxyalkanoic acid granules in *Alcaligenes eutrophus*. *J. Bacteriol. 177*, 2425–2435.
14. York, G. M., Stubbe, J., and Sinskey, A. J. (2001) New insight into the role of the PhaP phasin of *Ralstonia eutropha* in promoting synthesis of polyhydroxybutyrate. *J. Bacteriol. 183*, 2394–2397.
15. Stubbe, J., and Tian, J. (2003) Polyhydroxyalkanoate (PHA) homeostasis: The role of PHA synthase. *Nat. Prod. Rep. 20*, 445–457.
16. Jia, Y., Kappock, T. J., Frick, T., Sinskey, A. J., and Stubbe, J. (2000) Lipases provide a new mechanistic model for polyhydroxybutyrate (PHB) synthases: Characterization of the functional residues in *Chromatium vinosum* PHB synthase. *Biochemistry 39*, 3927–3936.
17. Jia, Y., Yuan, W., Wodzinska, J., Park, C., Sinskey, A. J., and Stubbe, J. (2001) Mechanistic studies on class I polyhydroxybutyrate (PHB) synthase from *Ralstonia eutropha*: Class I and III synthases share a similar catalytic mechanism. *Biochemistry 40*, 1011–1019.
18. Muh, U., Sinskey, A. J., Kirby, D. P., Lane, W. S., and Stubbe, J. (1999) PHA synthase from *Chromatium vinosum*: Cysteine 149 is involved in covalent catalysis. *Biochemistry 38*, 826–837.
19. Tian, J., Sinskey, A. J., and Stubbe, J. (2005) Detection of intermediates from the polymerization reaction catalyzed by a D302A mutant of class III polyhydroxyalkanoate (PHA) synthase. *Biochemistry 44*, 1495–1503.

20. Tian, J. M., Sinskey, A. J., and Stubbe, J. (2005) Class III polyhydroxybutyrate synthase: Involvement in chain termination and reinitiation. *Biochemistry 44*, 8369–8377.
21. Wodzinska, J., Snell, K. D., Rhomberg, A., Sinskey, A. J., Biemann, K., and Stubbe, J. (1996) Polyhydroxybutyrate synthase: Evidence for covalent catalysis. *J. Am. Chem. Soc. 118*, 6319–6320.
22. Gerngross, T. U., Snell, K. D., Peoples, O. P., Sinskey, A. J., Csuhai, E., Masamune, S., and Stubbe, J. (1994) Overexpression and purification of the soluble polyhydroxyalkanoate synthase from *Alcaligenes eutrophus*: Evidence for a required posttranslational modification for catalytic activity. *Biochemistry 33*, 9311–9320.
23. Liebergesell, M., Sonomoto, K., Madkour, M., Mayer, F., and Steinbuchel, A. (1994) Purification and characterization of the poly(hydroxyalkanoic acid) synthase from *Chromatium vinosum* and localization of the enzyme at the surface of poly(hydroxyalkanoic acid) granules. *Eur. J. Biochem. 226*, 71–80.
24. Liebergesell, M., and Steinbuchel, A. (1992) Cloning and nucleotide sequences of genes relevant for biosynthesis of poly(3-hydroxybutyric acid) in *Chromatium vinosum* strain D. *Eur. J. Biochem. 209*, 135–150.
25. Austin, M. B., and Noel, J. P. (2003) The chalcone synthase superfamily of type III polyketide synthases. *Nat. Prod. Rep. 20*, 79–110.
26. Smith, S. (1994) The animal fatty acid synthase: One gene, one polypeptide, seven enzymes. *FASEB J. 8*, 1248–1259.
27. Yuan, W., Jia, Y., Tian, J. M., Snell, K. D., Muh, U., Sinskey, A. J., Lambalot, R. H., Walsh, C. T., and Stubbe, J. (2001) Class I and III polyhydroxyalkanoate synthases from *Ralstonia eutropha* and *Allochromatium vinosum*: Characterization and substrate specificity studies. *Arch. Biochem. Biophys. 394*, 87–98.
28. Jencks, W. P., Cordes, S., and Carriuolo, J. (1960) The free energy of thiol ester hydrolysis. *J. Biol. Chem. 235*, 3608–3614.
29. Rehm, B. H., Antonio, R. V., Spiekermann, P., Amara, A. A., and Steinbuchel, A. (2002) Molecular characterization of the poly(3-hydroxybutyrate) (PHB) synthase from *Ralstonia eutropha*: In vitro evolution, site-specific mutagenesis and development of a PHB synthase protein model. *Biochim. Biophys. Acta 1594*, 178–190.
30. Ferrer, J. L., Jez, J. M., Bowman, M. E., Dixon, R. A., and Noel, J. P. (1999) Structure of chalcone synthase and the molecular basis of plant polyketide biosynthesis. *Nat. Struct. Biol. 6*, 775–784.
31. Tarshis, L. C., Yan, M. J., Poulter, C. D., and Sacchettini, J. C. (1994) Crystal Structure of Recombinant Farnesyl Diphosphate Synthase at 2.6-Angstrom Resolution. *Biochemistry 33*, 10871–10877.
32. Lawrence, A. G., Choi, J., Rha, C., Stubbe, J., and Sinskey, A. J. (2005) In vitro analysis of the chain termination reaction in the synthesis of poly-(R)-β-hydroxybutyrate by the class III synthase from *Allochromatium vinosum*. *Biomacromolecules 6*, 2113–2119.